

Fig. 2. The coding rules for proposed FPWM

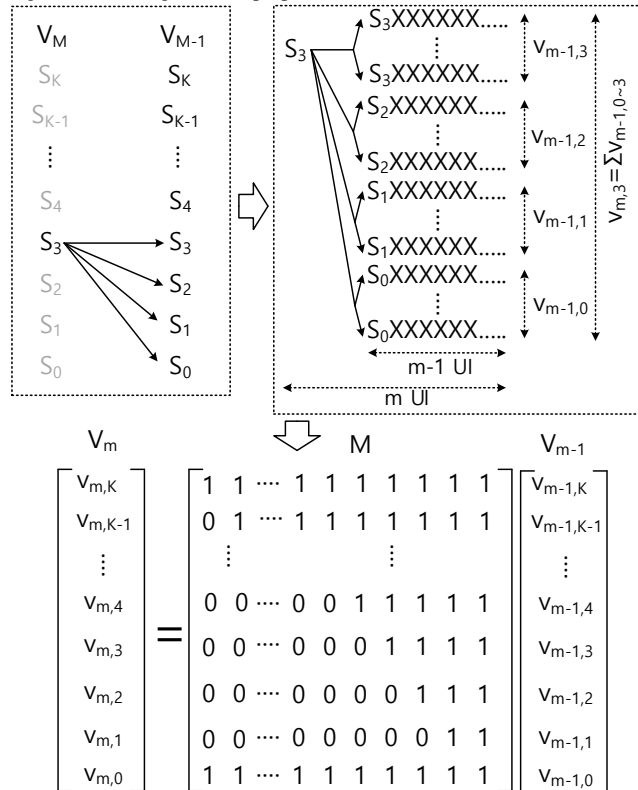


Fig. 3. The bitrate calculation for proposed FPWM

The number of possible symbol arrays in a frame satisfying these rules is derived as shown in Fig.3. The component value $v_{m,q}$ of vector V_m denotes the number of possible combinations of m symbol arrays starting with symbol 'S_q'. For example, if the frame length is 1 UI, only 'S₀' or 'S_K' symbol is possible. Therefore,

$$V_1 = [1 \ 0 \ 0 \ \dots \ 0 \ 1]^T \quad (1)$$

According to the rules in Fig.2, the number of symbol arrays of length m starting with 'S_q' is the sum of the number of symbol arrays of length $m-1$ starting with 'S₀' ~ 'S_q'. Then, the relationship between $v_{m,q}$ and $v_{m-1,q}$ can be expressed as follows.

$$v_{m,q} = \begin{cases} \sum_{h=0}^q v_{m-1,h} & (\text{if } q > 0) \\ \sum_{h=0}^K v_{m-1,h} & (\text{if } q = 0) \end{cases} \quad (2)$$

Eq.(2) can be expressed in a matrix form, and it is possible to derive V_m from V_1 as follows.

$$V_m = \begin{bmatrix} v_{m,K} \\ v_{m,K-1} \\ \vdots \\ v_{m,2} \\ v_{m,1} \\ v_{m,0} \end{bmatrix} = \begin{bmatrix} 1 & 1 & \dots & 1 & 1 & 1 \\ 0 & 1 & \dots & 1 & 1 & 1 \\ \vdots & \vdots & \ddots & \vdots & \vdots & \vdots \\ 0 & 0 & \dots & 1 & 1 & 1 \\ 0 & 0 & \dots & 0 & 1 & 1 \\ 1 & 1 & \dots & 1 & 1 & 1 \end{bmatrix} \begin{bmatrix} v_{m-1,K} \\ v_{m-1,K-1} \\ \vdots \\ v_{m-1,2} \\ v_{m-1,1} \\ v_{m-1,0} \end{bmatrix} = MV_{m-1} = M^{m-1}V_1 \quad (3)$$

The total number of symbol arrays that can be represented as one frame of FPWM with m UI length is $N = \sum_{h=0}^K v_{m,h}$ so that $\lceil \log_2 N \rceil$ bits can be encoded into the frame. The normalized bitrate of the

proposed FPWM scheme with the frame length of m UI and pulse width resolution of K is calculated as follows.

$$\text{bitrate} (\text{bit} / \text{UI}) = \frac{\lfloor \log_2 \sum_{h=0}^K v_{m,h} \rfloor}{m} \quad (4)$$

The normalized bitrate means the number of bits encoded per 1 UI. The normalized bitrates of the NRZ, PAM4, and the previously published FPWM scheme are 1, 2, and 1.33 bit/UI, respectively.[9] Fig.4 plots the normalized bitrates of the proposed FPWMs at various frame lengths and pulse width resolutions. It shows that the bitrate of the proposed FPWM at $m = 6$ and $K = 4$ is about 25% higher than the previous FPWM with the same frame length and pulse width resolution.

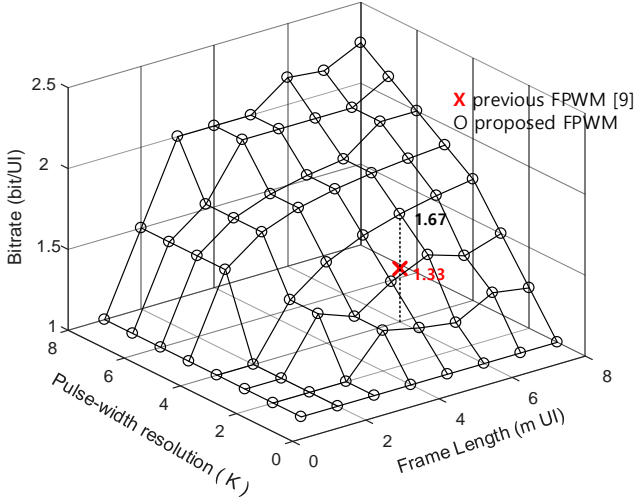


Fig. 4. The calculated bitrates of the proposed FPWMs with various Frame lengths and pulse width resolutions

B. Coding algorithm

The encoder converts the input binary data into its corresponding FPWM symbol array. The array composed of $K+1$ different symbols (' $S_0 \sim S_K$ ') can be regarded as a numeral system of radix $K+1$ with Least Significant Digit (LSD) on the right and Most Significant Digit (MSD) on the left. Table I shows an example of FPWM code with $K = 4$ corresponding to the input binary data. If the coding rule in Fig.2 is not applied, the encoder structure can be represented simply as a binary to the base-5 converter as shown in Fig.5. Conversion starts sequentially from the MSD. At each step, the input value is quantized to five levels. The result of the quantization in blue is then removed from the input, and the residual value passes to the next step for further quantization. Each step performs quantization independently of each other, enabling pipeline operation.

TABLE I
CODE TABLE OF THE PROPOSED FPWM ($K=4$)

Decimal	binary	FPWM	FPWM
	MSB→LSB	(w/o coding rule)	(with coding rule)
0	00...0000	$S_0 \dots S_0 S_0 S_0 S_0$	$S_0 \dots S_0 S_0 S_0 S_0$
1	00...0001	$S_0 \dots S_0 S_0 S_0 S_1$	$S_0 \dots S_0 S_0 S_0 S_4$
2	00...0010	$S_0 \dots S_0 S_0 S_0 S_2$	$S_0 \dots S_0 S_0 S_1 S_0$
3	00...0011	$S_0 \dots S_0 S_0 S_0 S_3$	$S_0 \dots S_0 S_0 S_2 S_0$
4	00...0100	$S_0 \dots S_0 S_0 S_0 S_4$	$S_0 \dots S_0 S_0 S_3 S_0$
5	00...0101	$S_0 \dots S_0 S_0 S_1 S_0$	$S_0 \dots S_0 S_0 S_4 S_0$
6	00...0110	$S_0 \dots S_0 S_0 S_1 S_1$	$S_0 \dots S_0 S_0 S_4 S_4$
7	00...0111	$S_0 \dots S_0 S_0 S_1 S_2$	$S_0 \dots S_0 S_1 S_0 S_0$
⋮	⋮	⋮	⋮

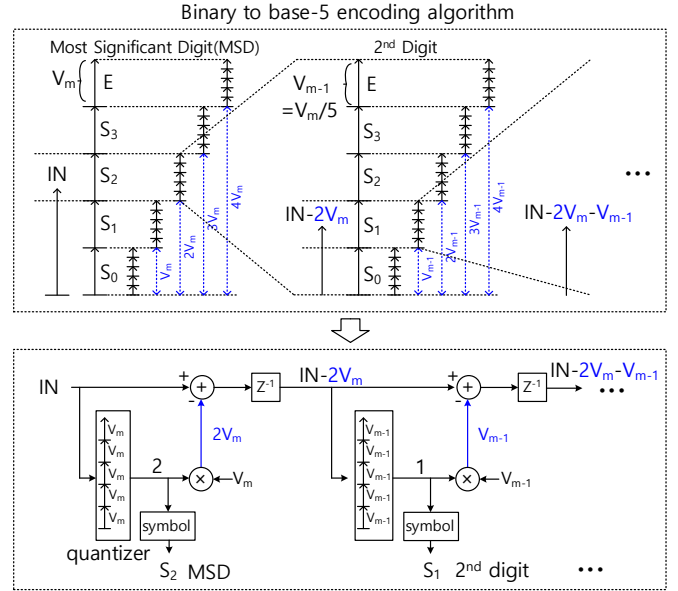


Fig. 5. Block diagram of binary to base-5 converting algorithm

However, if the coding rule in Fig.2 is applied, the forbidden transition should be excluded. Fig.6 shows the modified encoder structure. According to the coding rule, the number of possible symbols in the next digit depends on the quantization result of the current digit. However, by subtracting the quantization result from the input value by the quantity indicated by blue in Fig.6, it is possible to perform independent pipeline encoding operation for each digit. This independent pipeline operation dramatically reduces the size of the LUT for encoding and enables unified FPWM coding theory for various frame lengths and pulse width resolutions.

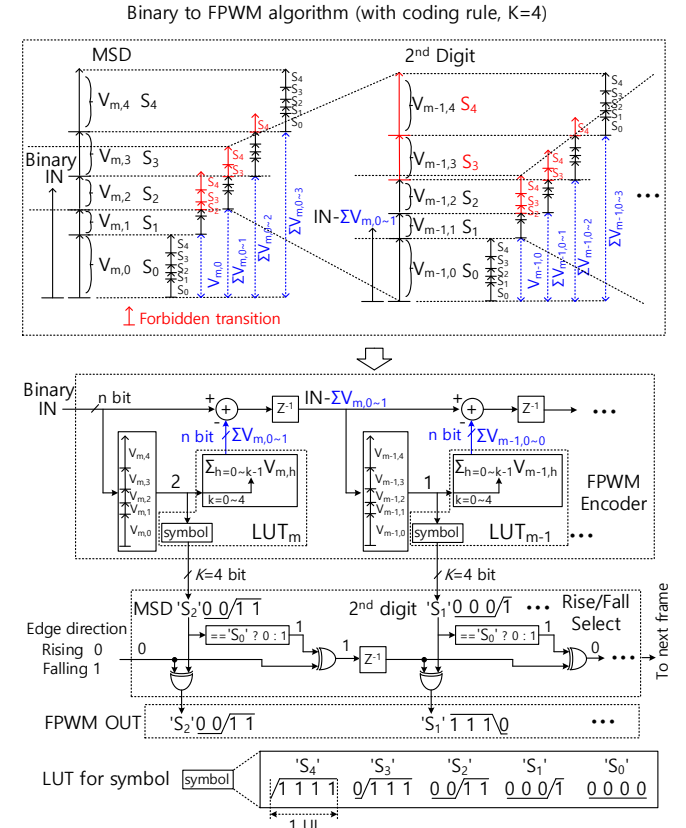


Fig. 6. Block diagram of encoding algorithm for FPWM with $K=4$

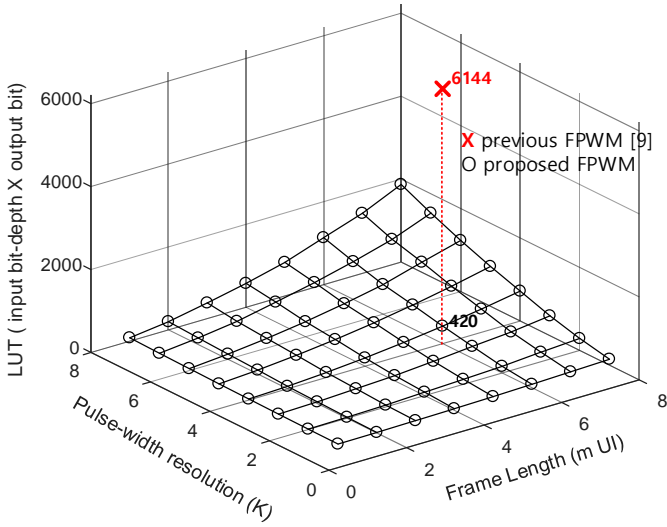


Fig. 7. The calculated LUT size required for encoding the proposed FPWMs with various Frame lengths and pulse width resolutions

The quantized results at each stage of the encoder are converted into FPWM symbols stored in the LUT. Each symbol requires K bits to represent K different edge phases. The symbols stored in the LUT have only rising edges. However, the rising and falling edges must alternate. Therefore, in order to transfer continuous FPWM symbols, the current symbol must be inverted to have the edge direction opposite to that of the previous symbol. The information of the edge direction of the current symbol is transmitted to the subsequent symbol while continuously toggling. This information transfer is performed between frames as well as symbols within a frame. However, if the current symbol is 'S₀', it means that there is no edge, so the information of the edge direction is transmitted to the next symbol without toggling. Then, the TX driver sends the connected FPWM symbols to the RX side.

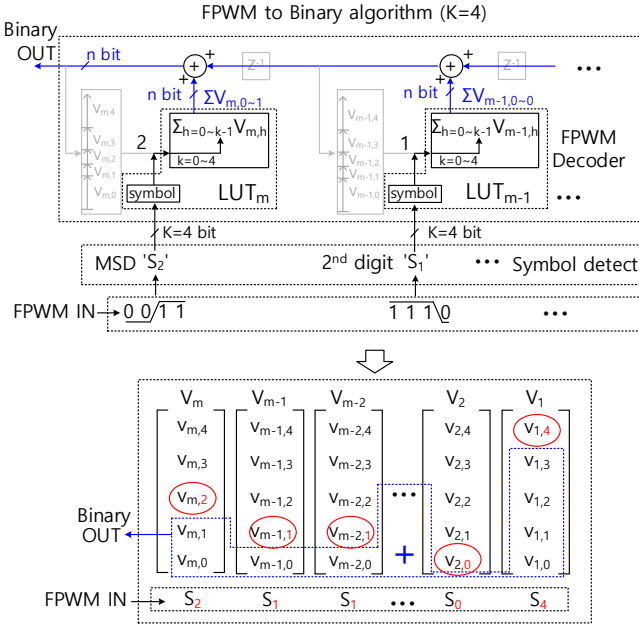


Fig. 8. Block diagram of decoding algorithm for FPWM with $K=4$

Fig.7 shows the size of LUTs required for encoding the proposed FPWMs of various frame lengths and pulse width resolutions. In the previous coding method, the LUT with 2^8 input bit-depth outputs 24 bits to convert 8-bit data to one frame of FPWM.[9] On the other hand,

the proposed FPWM with the same frame length ($m=6$ UI) and pulse width resolution ($K=4$) can encode 10 bits in one frame. Therefore, as shown in Fig.6, the input bit-depth of the LUT for one digit is $5(=K+1)$, and the LUT output is 14bit ($=n+K$). A total of six LUTs are required, from MSD to LSD. If the size of LUT is estimated as a product of input bit-depth and the number of output bits, the LUT size for the previous FPWM encoding scheme is $6144(=2^8 \times 24)$. However, the size of the LUT required for the proposed coding algorithm is $420(=5 \times 14 \times 6)$, which is about 93% smaller than the conventional FPWM. Since the LUT is the biggest bottleneck of the previous coding method, the significantly reduced LUT in size enables more complex FPWM coding with higher bitrates.

The decoding algorithm converts the input FPWM symbol array into the original binary data, and it can be implemented by inverting the encoding algorithm as shown in Fig.8. Therefore, the decoder only requires much smaller LUT than conventional methods. This decoding procedure can be understood as an operation of adding all the vector components $v_{m,q}$ below the row corresponding to the received symbol in each V_m vector, as shown in the lower part of Fig.8.

III. SIMULATION

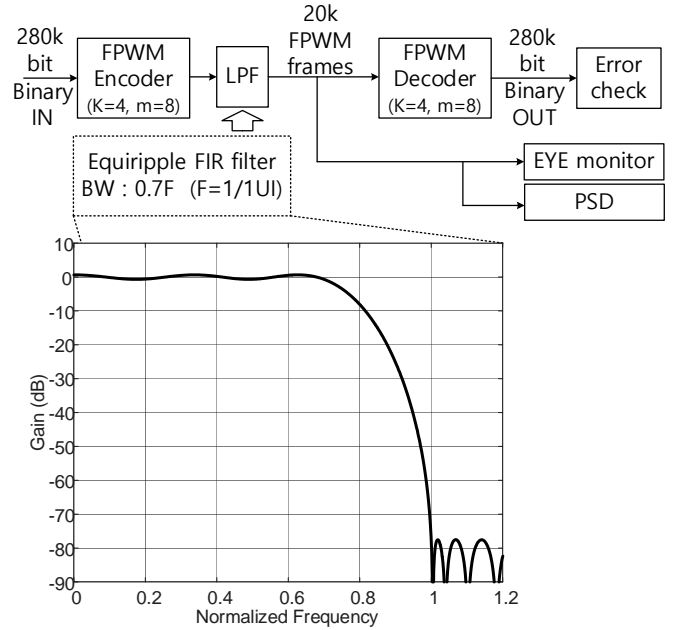


Fig. 9. MATLAB simulation setup

Fig.9 shows the MATLAB simulation setup to verify the proposed FPWM scheme and its coding algorithm. The frame length and the pulse width resolution are set to $m = 8$ UI and $K = 4$, respectively. The proposed coding algorithm can encode 14-bit data into 8 UI, so the bitrate is 1.75. A total of 280k bits is converted into 20k frames and then transmitted to the decoder. For comparison, 160k bits of data are also sent as NRZ signals with the same baud rate. Both of the encoded FPWM signal and the NRZ signal pass through an equiripple low pass filter (LPF) with a bandwidth of $0.7F$, where F is a normalized frequency with a period of one UI. Then, the decoder is fed the LPF output, recovering original binary data without bit errors. The transmitted FPWM signal provides the bitrate 75% greater than NRZ with the same bandwidth.

Fig.10 shows the eye-diagram and power spectral density (PSD) of the encoded FPWM signal. Since the last symbol of the frame is 'S₀' or 'S_K', the eye is open during the last 1 UI period of the frame. The PSD of the FPWM is lower than NRZ at DC and higher at mid frequencies.

This spectrum imbalance of FPWM is due to different probabilities between symbols. Table II shows the probabilistic ratio between the symbol 'S₀' and other symbols for various FPWMs. As the pulse width resolution increases, the total number of available symbols also increases, relatively lowering the probability of 'S₀'. Since all symbols except 'S₀' have edges, an increase in the probability of these symbols boosts the mid-frequency components of the FPWM signal.

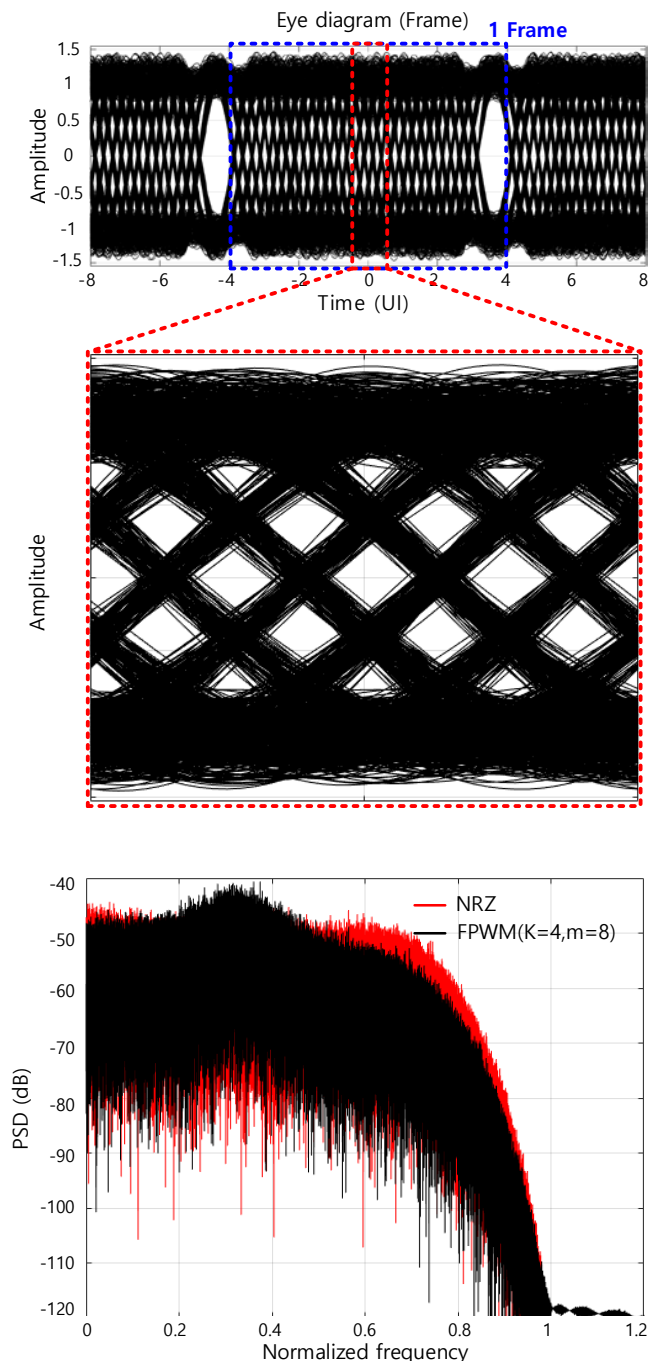


Fig. 10. Simulated eye-diagram and power spectral density

IV. CONCLUSION

This paper proposes a general FPWM scheme and its coding algorithm. The proposed FPWM scheme shows 25% higher bitrate than the previous FPWM at the same frame length and the pulse width resolution. Meanwhile, its encoding and decoding algorithms require 93% less LUT size than the prior art. The simple coding algorithm

derived from the unified FPWM theory enables designing and implementing other complex FPWMs having different frame lengths and pulse width resolutions. The FPWM encoder and decoder with longer frame length than previous FPWM were simulated as an example in MATLAB. In the simulation, 14bit was coded in 8UI to have bitrate close to PAM4. The received FPWM signals were successfully decoded without bit error, and their logical feasibility was verified.

TABLE II
THE PROBABILITY OF SYMBOLS FOR VARIOUS FPWMs

K	m	# of symbols in all possible arrays ($m \times N$)	# of S ₀ (no edge)	# of S _{1-K}
1*	8	2048	1024 (50%)	1024 (50%)
2	8	12776	5911(46.3%)	6865(53.7%)
3	8	47168	20636(43.8%)	26532(56.2%)
4	8	131944	55296(41.9%)	76648(58.1%)

* FPWM with $K=1$ is equivalent to NRZ.

REFERENCES

- [1] Y. Frans *et al.*, "A 56Gb/s PAM4 wireline transceiver using a 32-way time-interleaved SAR ADC in 16nm FinFET," *2016 IEEE Symposium on VLSI Circuits (VLSI-Circuits)*, Honolulu, HI, 2016, pp. 1-2.
- [2] J. Im *et al.*, "A 40-to-56Gb/s PAM-4 receiver with 10-tap direct decision-feedback equalization in 16nm FinFET," *2017 IEEE International Solid-State Circuits Conference (ISSCC)*, San Francisco, CA, 2017, pp. 114-115.
- [3] G. Steffan *et al.*, "A 64Gb/s PAM-4 transmitter with 4-Tap FFE and 2.26pJ/b energy efficiency in 28nm CMOS FDSOI," *2017 IEEE International Solid-State Circuits Conference (ISSCC)*, San Francisco, CA, 2017, pp. 116-117.
- [4] X. Zheng *et al.*, "A 4-40 Gb/s PAM4 transmitter with output linearity optimization in 65 nm CMOS," *2017 IEEE Custom Integrated Circuits Conference (CICC)*, Austin, TX, 2017, pp. 1-4.
- [5] K. Zheng *et al.*, "An Inverter-Based Analog Front End for a 56 GB/S PAM4 Wireline Transceiver in 16NMCOS," *2018 IEEE Symposium on VLSI Circuits (VLSI-Circuits)*, Honolulu, HI, 2018, pp. 269-270.
- [6] N. Kikuchi, R. Hirai and T. Fukui, "Non-linearity Compensation of High-Speed PAM4 Signals from Directly-Modulated Laser at High Extinction Ratio," *ECOC 2016; 42nd European Conference on Optical Communication*, Dusseldorf, Germany, 2016, pp. 1-3.
- [7] K. Maeda, T. Norimatsu, K. Kogo, N. Kohmu, K. Nishimura and I. Fukasaku, "An Active Copper-Cable Supporting 56-Gbit/s PAM4 and 28-Gbit/s NRZ with Continuous Time Linear Equalizer IC for to-Meters Reach Interconnection," *2018 IEEE Symposium on VLSI Circuits (VLSI-Circuits)*, Honolulu, HI, 2018, pp. 49-50.
- [8] Aurangozeb, A. D. Hossain, M. Mohammad and M. Hossain, "Channel-Adaptive ADC and TDC for 28 Gb/s PAM-4 Digital Receiver," *IEEE Journal of Solid-State Circuits*, vol. 53, no. 3, pp. 772-788, March 2018. DOI: 10.1109/JSSC.2017.2777099
- [9] S. Jeon *et al.*, "A 20Gb/s transceiver with framed-pulsewidth modulation in 40nm CMOS," *2018 IEEE International Solid - State Circuits Conference (ISSCC)*, San Francisco, CA, 2018, pp. 270-272.